A Modified Approach to Induce Predictable Congestive Heart Failure by Volume Overload in Rats

Sascha Treskatsch[1,9], Aarne Feldheiser[1,9], Adrian T. Rosin[1], Marco Sifringer[1], Helmut Habazettl[2], Shaaban A. Mousa[1], Mehdi Shakibaei[3], Michael Schäfer[1], Claudia D. Spies[1]*

1 Department of Anesthesiology and Intensive Care Medicine, Campus Charité, Mitte and Campus Virchow-Klinikum, Charité - Universitätsmedizin Berlin, Berlin, Germany, 2 Institute of Physiology, Campus Charité Mitte, Charité - Universitätsmedizin Berlin, Berlin, Germany, 3 Institute of Anatomy, Ludwig-Maximilians-Universität München, München, Germany

Abstract

The model of infrarenal aortocaval fistula (ACF) has recently gained new interest in its use to investigate cardiac pathophysiology. Since in previous investigations the development of congestive heart failure (CHF) was inconsistent and started to develop earliest 8–10 weeks after fistula induction using a 18G needle, this project aimed to induce a predictable degree of CHF within a definite time period using a modified approach. An aortocaval fistula was induced in male Wistar rats using a 16G needle as a modification of the former 18G needle-technique described by Garcia and Diebold. Results revealed within 28 ± 2 days of ACF significantly increased heart and lung weight indices in the ACF group accompanied by elevated filling pressure. All hemodynamic parameters derived from a pressure-volume conductance-catheter *in vivo* were significantly altered in the ACF consistent with severe systolic and diastolic left ventricular dysfunction. This was accompanied by systemic neurohumoral activation as demonstrated by elevated rBNP-45 plasma concentrations in every rat of the ACF group. Furthermore, the restriction in overall cardiac function was associated with a β1- and β2-adrenoreceptor mRNA downregulation in the left ventricle. In contrast, β3-adrenoreceptor mRNA was upregulated. Finally, electron microscopy of the left ventricle of rats in the ACF group showed signs of progressive subcellular myocardial fragmentation. In conclusion, the morphometric, hemodynamic and neurohumoral characterization of the modified approach revealed predictable and consistent signs of congestive heart failure within 28 ± 2 days. Therefore, this modified approach might facilitate the examination of various questions specific to CHF and allow for pharmacological interventions to determine pathophysiological pathways.

Introduction

Despite improvements in the treatment of congestive heart failure (CHF), CHF is still associated with a high mortality. The overall prevalence of CHF is still increasing because of the ageing of the population and the success in prolonging survival in patients suffering cardiac disease [1]. Therefore, the number of patients with CHF scheduled for surgery with a consecutive increase in the perioperative risk, especially in high-risk-procedures, e.g. vascular and cardiothoracic surgery, is growing. However, knowledge about the underlying pathophysiological mechanisms, which promote heart failure in the perioperative course resulting in biventricular volume overload remains scarce. Thus, it would be of advantage to have a reproducible and predictable experimental model of heart failure developing within a brief time period.

CHF is a multicausal state in which the heart is unable to deliver an appropriate amount of substrates and oxygen to the tissues [2]. This has been reflected in several experimental animal models with distinct pathophysiological causes: a) coronary ligation – loss of cardiomyocytes, b) aortic banding – pressure overload, c) salt sensitive hypertension – pressure overload, d) genetic models – loss of cardiomyocytes or pressure/volume overload, e) toxic cardio-myopathies – loss of cardiomyocytes [3] and finally f) infrarenal aortocaval fistula (ACF) – volume overload [4].

The experimental model of volume overload induced by an aortocaval fistula was first published by Holman in 1937 and has been established with slight modifications by Garcia and Diebold since 1990 [5]. However, in previous investigations of ACF induced volume overload, heart failure was inconsistent and started to develop earliest 8–10 weeks after fistula induction using a 18G-needle [4,6]. In a study by Melenovsky et al. overt signs of CHF became first obvious at approximately 20 weeks after ACF placement in male Wistar rats [7] and were only present in 65% at the 22th week [8].

Therefore, in this project we aimed to induce a predictable degree of CHF in every animal within a definite time period using a modified approach (16G needle) of the previously published 18G needle-technique by Garcia and Diebold [5]. Such a model would facilitate the examination of various questions specific to CHF and would allow for precisely timed pharmacological interventions to determine pathophysiological pathways. 28 ± 2 days after ACF induction, the extent of heart failure was determined morpholog-

Table 1. Morphometric data.

	Control (n = 6)	ACF (n = 6)
BW (g)	370±16 (330–419)	366±9 (345–395)
Heart (mg)	1410±49 (1270–1570)	2430±113 (2000–2730)*
Heart/BW (mg/g BW)	3.9±0.1 (3.5–4.1)	6.6±0.2 (5.7–7.0)*
Lung (mg)	1370±43 (1270–1490)	2675±204 (1930–3170)*
Lung/BW (mg/g BW)	3.8±0.2 (3.2–4.5)	7.3±0.6 (5.6–9.1)*
Kidney (mg)	1192±60 (1050–1340)	1160±62 (950–1330)
Kidney/BW (mg/g BW)	3.3±0.1 (3.1–3.5)	3.2±0.1 (2.8–3.4)
Liver (mg)	12824±877 (10620–15070)	13707±976 (10350–16500)
Liver/BW (mg(g BW)	35.0±1.6 (30.5–40.3)	37.4±2.4 (30.0–45.8)

Values are means ± SEM and range; n = 6 rats/group. BW, body weight.
*indicates a statistically significant difference betwenn groups (p<0.001).
doi:10.1371/journal.pone.0087531.t001

ically, and hemodynamically by means of an intraventricular pressure-volume conductance catheter. Specific adaptations in BNP plasma concentrations and the expression of the β1-, β2- and β3-adrenoreceptor mRNA expression were examined in this modified ACF model. Finally, electron microscopy should reveal subcellular changes according to CHF.

Materials and Methods

Animals

Male Wistar rats, 280–300 g (Harlan Winkelmann, Borchen, Germany), were maintained on standard laboratory rat chow and water ad libitum. The animals were kept on a 12-h light–dark cycle. This study was carried out in strict accordance with the recommendations in the Guide for the Care and Use of Laboratory Animals of the National Institutes of Health. The protocol was approved by the Committee on the Ethics of Animal Experiments of the local care authories (Landesamt für Gesundheit und Soziales, Berlin, Germany) (Permit Number: G 0119/08). All surgery was performed under isoflurane (ACF induction) and tiletamine/zolazepam (hemodynamic measurements) anesthesia, and all efforts were made to minimize suffering. Post surgical analgesia was provided by metamizole (40 mg/kg s.c.).

Experimental model

The needle-technique to induce an infrarenal aortocaval fistula (ACF) has previously been described by Garcia and Diebold using a 18G needle [5]. Here, we modified this technique using a 16G needle. Briefly, a laparotomy was performed and the aorta was punctured with a 16G disposable needle (Braun, Melsungen, Germany) distal to the renal arteries. Then, the needle was advanced through the aortic wall into the adjacent inferior vena cava. After temporarily compressing the aorta and venous vessels above and below the puncture site, the needle was carefully withdrawn and the aortic puncture site was sealed with a drop of cyanoacrylate glue. Patency of the fistula ACF was visualized by the pulsatile flow of oxygenated blood into the vena cava inferior from the infrarenal aorta [9]. Vessels of sham-operated control animals were also temporarily compressed and glued together, but without any puncture of the aorta.

Hemodynamic measurements

For hemodynamic measurements the "closed chest" method in spontaneously breathing rats was used as described earlier [10]. All measurements were performed under tiletamine/zolazepam anesthesia (Zoletil®, 10 mg/kg s.c. followed by 50 mg/kg i.m.) 28±2 days after fistula induction [11]. The rats were placed on a heating pad to maintain body temperature. After tracheotomy a PE-50 tubing catheter was inserted via the left jugular vein into the superior vena cava for assessment of central venous pressure. Arterial blood pressure was measured by cannulating the right carotid artery with a micro-tip pressure-volume conductance catheter (Millar®, SPR-838 NR). By further advancing the catheter into the left ventricle intraventricular pressures and volumes were registered. The position of the catheter was optimized aiming for maximal stroke volume (SV). For measurement of the parallel conductance volume 100 µl of 15% saline were injected into the central venous line to determine the correction factor for the blood-LV tissue interface, however, inhomogeneity of the electric field was not corrected. Heart rate was derived from the ECG signal. After completion of cannulation there was a 10–15 minute equilibration period before starting the measurements. All measurements were performed in spontaneously breathing rats without mechanical ventilation. All signals were recorded and analyzed by the PowerLab®-system and software (ADInstruments, Dunedin, New Zealand). After completion of the hemodynamic measurements animals were killed by exsanguination and organs were eviscerated for further determinations.

Determination of BNP plasma concentration

Blood samples for rat brain natriuretic peptide 45 (rBNP-45) determinations were withdrawn from control (n = 6) and ACF (n = 6) animals into EDTA-preloaded tubes after completion of hemodynamic measurements. The blood was centrifuged at 4°C at 1,000 g for 10 min immediately after withdrawal, and the plasma was maintained at −80°C until extraction. Plasma rBNP-45 concentrations were measured by using a sensitive enzyme-linked immunosorbent assay (ELISA) kit (Abnova, Heidelberg, Germany) [12].

β1-, β2- and β3-adrenoreceptor RT-PCR

Tissue of the left ventricle for determination of β1-, β2- and β3-adrenoreceptor (AR) mRNA was obtained from sham-operated control (n = 6) and ACF (n = 6) animals after completion of hemodynamic measurements. Following mRNA extraction from rat cardiac tissue reverse transcription-polymerase chain reaction (RT-PCR) analysis was performed as described previously [13]. In brief, total RNA was prepared with the commercially available kit Qiazol Lysis Reagent, (Qiagen, Hilden, Germany) according to the manufacturer's protocol. Then, 1 µg RNA determined by Nanodrop (Peqlab, Erlangen, Germany) were used for transcription to cDNA by using the Omniscript RT Kit (Qiagen) as follows: 0.5 mM dNTP, 5 µM random primer, 10 U RNase Inhibitor, and 4 U Omniscript reverse Transcriptase. Samples were incubated at 42°C for 1 hour, and cDNA was stored at −20°C. The following primers were used: 5′-CTGCTACAACGACCCCAAGTG-3′ (forward) and 5′-AACACCCGGAGGTACACGAA-3′ (reverse) for β1-AR [14], 5′-GAGCCACACGGGAATGACA-3′ (forward) and 5′-CCAGGCGATAACCGACATGA-3′ (reverse) for β2-AR [14] and 5′-GCCGAGACTACAGACCATAACCA-3′ (forward) and 5′-CATTACGAGGAGTCCCACTACCA-3′ (reverse) for β3-AR [15]. Taqman qRT-PCR was performed with a SYBR Green kit following the manufacturer's instructions (Applied Biosystems, Foster City, CA). Experiments were repeated three

A

B
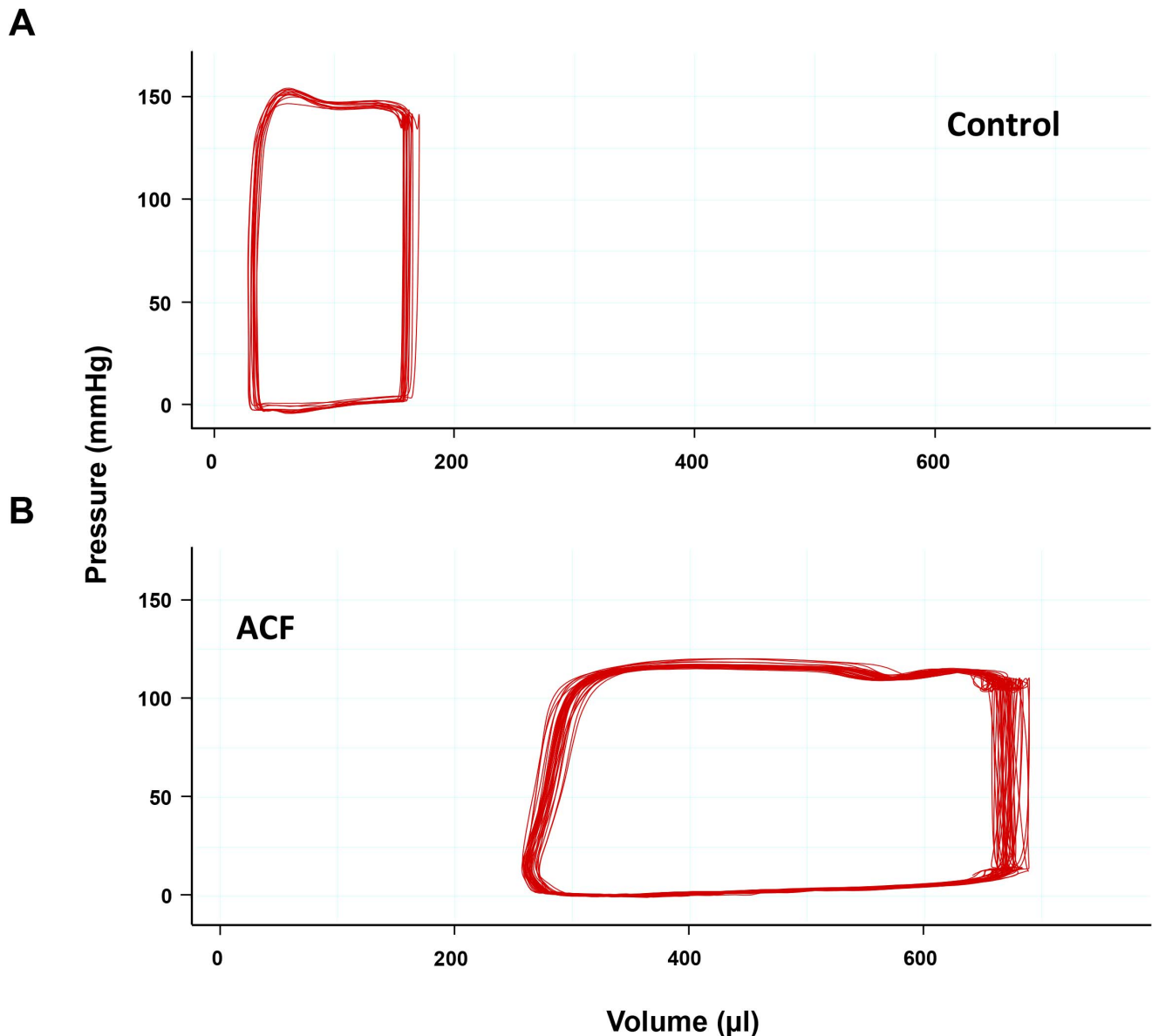
Figure 1. Representative pressure-volume loops of a sham-operated control rat (top) and an ACF rat (bottom).
doi:10.1371/journal.pone.0087531.g001

times. β1-, β2- and β3-AR mRNA was quantified by using triplicates of samples with the ABI Prism 7500 sequence detection system (Applied Biosystems, System Software v 1.3.1.) and the delta-delta CT method. The housekeeping gene 18S rRNA (5′-CGGCTACCACATCCAAGGAA-3′ forward and 5′-GCTGGAATTACCGCGGCT-3′ reverse) was used as an internal reference gene.

Electron microscopy

Rats of each group were anesthetized with tiletamine/zolazepam (Zoletil®) (see above) and transcardially perfused with 100 ml warm saline, followed by 300 ml 4% paraformaldehyde/0.1% glutaraldehyde/0.2% picric acid solution (pH 7.4) in 0.16 M phosphate buffer solution (pH 7.4). After perfusion the hearts were removed and postfixed for 3 hours at 4°C in the fixative solution. Tissue of the left ventricle was processed for electron microscopy as described previously [16].

Statistical analysis

All tests were performed using SPSS 20.0 software program. Normal distribution was analyzed with the Kolmogorov-Smirnov test. Results are expressed as means ± SEM or median and interquartile distance. Statistical significance between the two groups was analyzed by Student t-test or Mann-Whitney test as appropriate. $P < 0.05$ was considered statistically significant.

Results

Increased heart and lung weight indices in rats with aortocaval fistula

Values for organ weight, body weight, and the organ weight/body weight ratio ("index") are given in Table 1. Body weights were not significantly different between the control and the ACF group 28±2 days after fistula induction. However, heart and lung weight indices were significantly increased (p<0.01) at 28±2 days

Table 2. Hemodynamic data.

	Control (n = 6)	ACF (n = 6)
HR (min^{-1})	386±13 (345–420)	345±14 (301–373)
SBP (mmHg)	155±7 (131–180)	122±6 (106–148)*
DBP (mmHg)	114±9 (72–134)	69±2 (63–76)*
LVEDP (mmHg)	5.0±0.3 (3.9–6.3)	13.9±1.3 (9.9–16.7)*
CVP (mmHg)	0.2±0.1 (0.0–0.7)	6.4±0.8 (3.6–8.4)*
dP/dt max. (mmHg/s)	15876±1128 (12143–18562)	9024±1207 (5616–13974)*
dP/dt min. (mmHg/s)	−9675±880 (−13344−−7715)	−5791±702 (−8714−−3614)*
Tau (ms)	8.0±0.4 (6.80–9.53)	13.4±1.1 (9.71–17.87)*
Elastance (mmHg/µl)	1.01±0.11 (0.68–1.32)	0.38±0.03 (0.31–0.48)*
LVEDV (µl)	188±8 (166–220)	633±51 (403–736)*
LVESV (µl)	48±2 (41–56)	400±38 (251–508)*
SV (µl)	140±7 (125–170)	233±24 (152–334)*
CO (ml/min)	54±4 (46–71)	81±10 (46–121)*
LVEF (%)	74±1 (72–77)	37±2 (30–45)*

Values are means ± SEM and range; n = 6 rats/group. BW, body weight.
*indicates a statistically significant difference between groups (*p*<0.05).
HR = heart rate; SBP = systolic blood pressure; DBP = diastolic blood pressure; LVEDP = left ventricular enddiastolic pressure; CVP = central venous pressure; dP/dt max. = maximum rate of pressure change of the left ventricle in systole; dP/dt min. = minimum rate of pressure change of the left ventricle in diastole; Tau = isovolumic relaxation constant; LVEDV = left ventricular enddiastolic volume; LVESV = left ventricular endsystolic volume; SV = stroke volume; CO = cardiac output; LVEF = left ventricular ejection fraction.
doi:10.1371/journal.pone.0087531.t002

after induction of the aortocaval fistula. Considering technical aspects of the here presented approach, the main complication was uncontrollable bleeding at the puncture site at ACF induction. However, after a learning phase (approximately 30 animals) which resulted in proper needle handling, i.e a) careful puncture of the anterior aortic wall not injuring the posterior wall, and b) very gentle advancement of the needle into the vena cava inferior,

perioperative mortality was <1%. During progression into heart failure 28±2 days mortality in a cohort of 23 animals was 17% (n = 4). Out of the remaining 19 rats n = 6 sham rats and n = 6 ACF rats were used for the morphometric, hemodynamic, neurohumoral, and beta-adrenergic mRNA measurements. In addition, n = 2 sham rats and n = 5 ACF rats were used for electron microscopy.
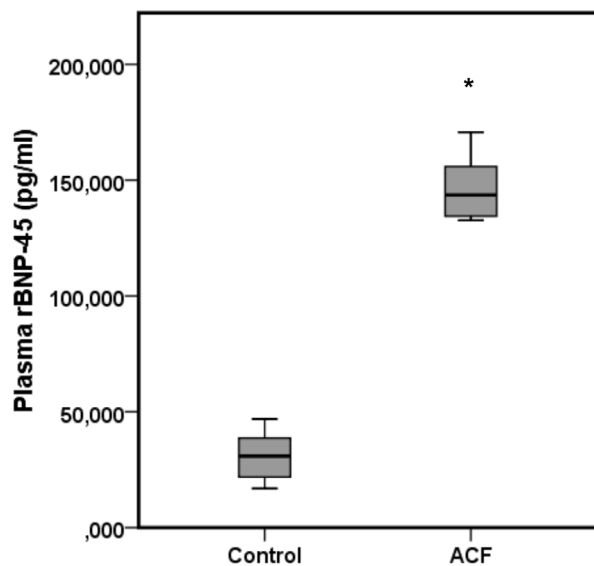
Systolic and Diastolic Dysfunction in ACF rats

Values for various hemodynamic parameters of the control and ACF groups are shown in Table 2. Central venous (CVP) and left end-diastolic pressure (LV-EDP) were significantly increased in ACF rats (p<0.01). Systolic and diastolic arterial blood pressures (SBP, DBP) were significantly reduced due to afterload reduction in rats with an aortocaval fistula (p<0.01). Cardiac output was nearly doubled in the ACF group. This was based on a nearly doubled stroke volume (p<0.01) forming a characteristic pressure-volume-loop in fistula-operated animals (Fig. 1 A and B). Left ventricular end-diastolic and end-systolic volumes (LVEDV, LVESV) were significantly higher than in the control group (p< 0.01). However, left ventricular ejection fraction (LVEF) (p<0.01) and the maximum rate of pressure development (p<0.01) were significantly reduced. There was no overlap in the data distribution between a) ACF rats with increased heart and lung weight indices and decreased LVEF and b) control rats. Furthermore, a slowed cardiac relaxation became apparent as a reduced maximum rate of pressure decay (p<0.01) and prolonged time of Tau (p<0.01).

Increased rBNP-45 plasma concentration in rats with heart failure

Values for the rBNP-45 plasma concentration from the control and ACF groups are shown in Figure 2. rBNP-45 plasma concentrations were significantly increased in the ACF group.

Figure 2. Total rBNP-45 plasma concentrations of control and ACF rats. There was no overlap in data distribution meaning ACF animals could be clearly distinguished from healthy animals. * indicates a statistically significant difference between both groups (p<0.01, n = 6 per group).
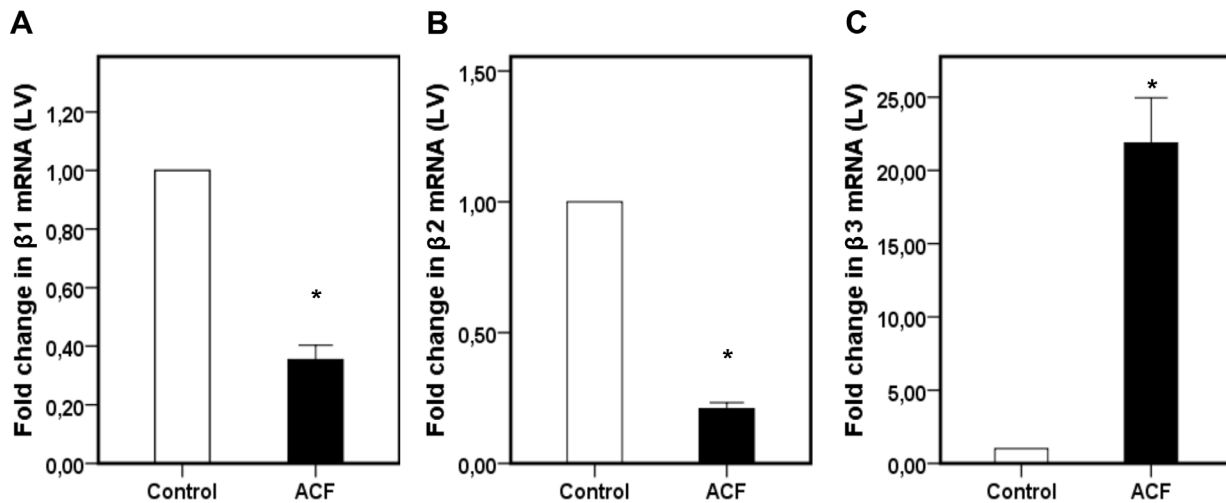doi:10.1371/journal.pone.0087531.g002

Figure 3. Fold change in β1- (A), β2- (B) and β3- (C) AR mRNA expression in the left ventricle of control and ACF rats. * indicates a statistically significant difference between both groups (p<0.01, n=6 per group).
doi:10.1371/journal.pone.0087531.g003

Again, there was no overlap in data distribution between control rats and ACF rats.

β1- and β2-AR mRNA downregulation in the LV

Values for the $\beta1$-, $\beta2$- and $\beta3$-adrenoreceptor mRNA from the control and fistula groups are shown in Figure 3. $\beta1$- and $\beta2$-adrenoreceptor mRNA expression was significantly decreased in the fistula group (p<0.01) (Fig. 3 A and B).

β3-AR upregulation 28 days after shunt induction

In contrast to the significant downregulation of $\beta1$- and $\beta2$-adrenoreceptor mRNA in the left ventricle (LV) of rats 28±2 days after shunt induction, $\beta3$-adrenoreceptor mRNA of the LV was significantly upregulated in rats with an aortocaval fistula (p<0.01) (Fig. 3 C).

Signs of progressive subcellular fragmentation in the myocardium of rats with an aortocaval fistula

A representative example of the changes of the subcellular myocardial structure is given in Figure 4. The electron microscopy image of the LV of rats in the ACF group showed: a) fragmented nuclear chromatin, b) reduced size of myofibrils, c) swollen mitochondria, d) vacuolization, e) dissolved cell-cell-contacts with degenerative appearances, and f) immigration of phagocytic leukocytes. This might suggest apoptotic changes in the left ventricle myocardium during the progressive course of heart failure.

Discussion

In previous publications heart failure was inconsistent and started to develop earliest ≥8 weeks after fistula induction using a 18G-needle [4,6]. Therefore, our goal was to modify the needle-technique to achieve a predictable CHF within a short time period to facilitate interventional studies with an improved assay
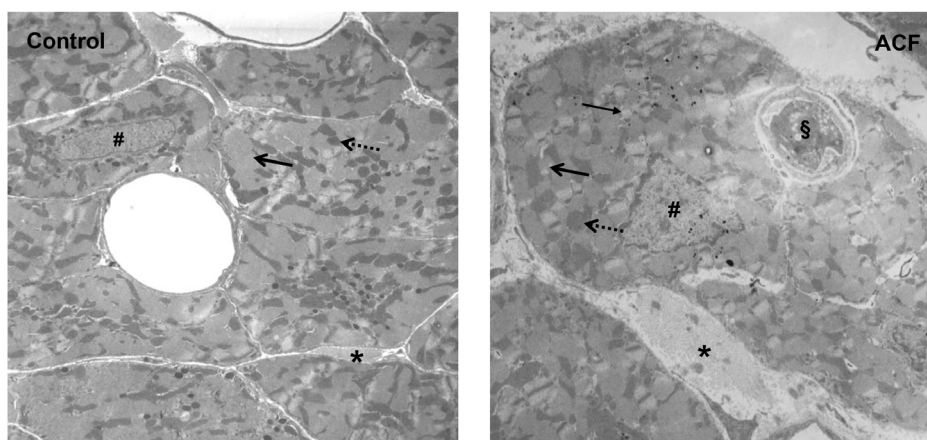
Figure 4. Electron microscopy in rats 4 weeks after induction of an aortocaval shunt (right) showing a) fragmented nuclear chromatin (#), b) reduced size of myofibrils ( ), c) swollen mitochrondria (←), d) vacuolization (→), e) dissolved cell-cell-contacts with degenerative appearances (*) and f) immigration of phagocytic leukocytes (§). Magnification: ×10.000.
doi:10.1371/journal.pone.0087531.g004

sensitivity. In this context, we used a 16G instead of a 18G needle, which theoretically resulted in 69% larger cross-sectional area of the fistula inducing a more pronounced cardiac volume overload to hasten the pathophysiological processes. In animals of the 16G needle ACF group, our findings met criteria to characterize a severe CHF already after 28 days: 1) LV end-diastolic volume > 550 µl [4], 2) lung mass >2500 mg [6,17], 3) significant increase (>50%) in heart weight to body weight ratio compared with the control group and/or a heart weight index ≥5,0 mg/g BW [17,18], and 4) elevated central venous pressure ≥4 mmHg [18]. As a new finding and in contrast to the previous studies using different fistula induction methods, e.g. microsurgery vs. different sized needles [4,9,19–21], these end points were reached within 4 weeks in every single rat of the here presented ACF group.

In vivo hemodynamic assessment of rats by means of a pressure-volume catheter has become the gold standard - besides echocardiography - in experimental models investigating adaptive changes due to myocardial infarction [22] or volume overload [23]. In using this modified approach, a complete hemodynamic characterization derived from a conductance catheter *in vivo* in this modified approach is shown for the first time. Intraventricular pressures and volumes in the control group were comparable to values previously published for healthy rats [10,23,24]. A nearly two-fold increase in the lung weight index accompanied by elevated central venous and left end-diastolic pressures denotes backward failure ("pulmonary congestion"). Finally, we demonstrated a clear separation between an increased heart and lung weight indices and a reduced LVEF in every ACF animal compared to every animal in the control group. This clearly depicts the transition from eccentric hypertrophy with preserved cardiac function to severe biventricular dilatation with decompensated heart failure due to pronounced volume overload in our modified approach [4,7,25,26].

Today, progressive heart failure has been recognized to develop from a combination of genetic, neurohumoral, inflammatory [27], and biochemical factors. Therefore, biomarkers have become important for clinical risk stratification. Beside Troponin in the case of acute coronary syndrome [28], BNP is one of the most interesting biomarkers to grade the extent of heart failure to support medical decisions making and to monitor responses to therapy [29,30]. An increase in BNP plasma concentration reliably reflects the neurohumoral activation due to persistent hemodynamic overload of the heart [31]. 28±2 days after fistula induction BNP plasma concentrations were significantly increased in our modified experimental model. This is consistent with previous results by Langenickel et al. demonstrating the superiority of cardiac BNP mRNA expression as a marker of the transition from compensated to overt heart failure in volume overloaded rats [17].

Also, subcellular fragmentation consistent with apoptotic changes of the myocardium has been recognized as an important pathophysiological mechanism promoting progression of heart failure [32–34]. This holds true for several causes of heart failure, including myocardial infarction [35], and pressure [36] and

volume overload [37]. As an additional new finding in our modified experimental approach, we were able to demonstrate sites of severe subcellular fragmentation in cardiomyocytes of the left ventricle 28±2 days after fistula induction. This is extending previous findings which demonstrated a) increased apoptotic rate of the myocardium only 16 weeks after ACF induction using a 18G needle [37], and b) mainly in non-cardiomyocytes [38]. However, further studies have to confirm these data.

Abnormalities in myocardial catecholamine release and in β-adrenergic receptor (AR) density in patients with congestive heart failure have long been recognized [39,40]. Adrenergic over-activity is one of the hallmarks of the heart failure syndrome and is associated with a poor prognosis [41–43]. As early as 1992, Hammond et al. reported blunted heart rate responsiveness to β1-AR stimulation in volume overloaded pigs due to β1-AR downregulation 5 weeks after fistula induction [44]. In failing human myocardium, β1-ARs are downregulated as studied with quantitative polymerase chain reactions in dilated and ischemic cardiomyopathy [45]. Also, Ihl-Vahl et al. were able to describe a decrease in mRNA-levels of beta 2-adrenergic receptors in the failing human heart [46]. In our results we demonstrate a β1- and β2-adrenoreceptor mRNA downregulation in the LV in rats with heart failure.

Almost two decades ago, the β3-adrenorecptor (β3-AR) has been identified in myocardial tissue [47]. In healthy myocardial tissue from rodents or humans, the mainly Gi-protein coupled β3-AR is only scarcely expressed. However, according to current knowledge [48–50], the β3-AR is upregulated in the failing heart of the ACF group which is consistent with our data from the ACF group.

In conclusion, our modified experimental model of heart failure using a 16G needle to induce an infrarenal aortocaval fistula has major advantages to investigate cardiac pathophysiology: congestive heart failure can reproducibly be induced within a relatively short and convenient time period. Combining morphometric, hemodynamic and biochemical parameters, the extent of heart failure can be well characterized. This modified model might facilitate the examination of various questions concerning CHF specifically by precisely timed interventions to determine pathophysiological pathways.

Acknowledgments

Author Contributions

Conceived and designed the experiments: AF M. Schäfer CDS. Performed the experiments: ST ATR. Analyzed the data: ST HH M. Schäfer. Contributed reagents/materials/analysis tools: M. Sifringer SAM M. Shakibaei CDS. Wrote the paper: ST M. Schäfer. Provided technical advice: AF HH.

References

1. McMurray JJV, Adamopoulos S, Anker SD, Auricchio A, Böhm M, et al. (2012) ESC Guidelines for the diagnosis and treatment of acute and chronic heart failure 2012: The Task Force for the Diagnosis and Treatment of Acute and Chronic Heart Failure 2012 of the European Society of Cardiology. Developed in collaboration with the Heart Failure Association (HFA) of the ESC. Eur J Heart Fail 14:803–869.

2. Ho KK, Pinsky JL, Kannel WB, Levy D (1993) The epidemiology of heart failure: the Framingham Study. J Am Coll Cardiol 22: 6A–13A.

3. Hasenfuss G (1998) Animal models of human cardiovascular disease, heart failure and hypertrophy. Cardiovasc Res 39: 60–76.

4. Brower GL, Henegar JR, Janicki JS (1996) Temporal evaluation of left ventricular remodeling and function in rats with chronic volume overload. Am J Physiol 271: H2071–2078.

5. Garcia R, Diebold S (1990) Simple, rapid, and effective method of producing aortocaval shunts in the rat. Cardiovasc Res 24: 430–432.

6. Wang X, Ren B, Liu S, Sentex E, Tappia PS, et al. (2003) Characterization of cardiac hypertrophy and heart failure due to volume overload in the rat. J Appl Physiol 94: 752–763.

7. Melenovsky V, Skaroupkova P, Benes J, Torresova V, Kopkan L, et al. (2012) The course of heart failure development and mortality in rats with volume overload due to aorto-caval fistula. Kidney Blood Press Res 35: 167–173.

8. Melenovsky V, Benes J, Skaroupkova P, Sedmera D, Strnad H, et al. (2011) Metabolic characterization of volume overload heart failure due to aorto-caval fistula in rats. Mol Cell Biochem 354: 83–96.

9. Dent MR, Tappia PS, Dhalla NS (2010) Gender differences in apoptotic signaling in heart failure due to volume overload. Apoptosis 15: 499–510.

10. Pacher P, Nagayama T, Mukhopadhyay P, Bátkai S, Kass DA (2008) Measurement of cardiac function using pressure-volume conductance catheter technique in mice and rats. Nat Protoc 3: 1422–1434.

11. Saha DC, Saha AC, Malik G, Astiz ME, Rackow EC (2007) Comparison of cardiovascular effects of tiletamine-zolazepam, pentobarbital, and ketamine-xylazine in male rats. J Am Assoc Lab Anim Sci 46: 74–80.

12. Heidrich K, Zhang K, Estrada M, Huang Y, Giordano FJ, et al. (2008) Chromogranin B regulates calcium signaling, nuclear factor kappaB activity, and brain natriuretic peptide production in cardiomyocytes. Circ Res 102: 1230–1238.

13. Mousa SA, Shaqura M, Schäper J, Treskatsch S, Habazettl H, et al. (2011) Developmental expression of δ-opioid receptors during maturation of the parasympathetic, sympathetic, and sensory innervations of the neonatal heart: early targets for opioid regulation of autonomic control. J Comp Neurol 519: 957–971.

14. Sato S, Nomura S, Kawano F, Tanihata J, Tachiyashiki K, et al. (2008) Effects of the beta2-agonist clenbuterol on beta1- and beta2-adrenoceptor mRNA expressions of rat skeletal and left ventricle muscles. J Pharmacol Sci 107: 393–400.

15. Hatakeyama Y, Sakata Y, Takakura S, Manda T, Mutoh S (2004) Acute and chronic effects of FR-149175, a beta 3-adrenergic receptor agonist, on energy expenditure in Zucker fatty rats. Am J Physiol Regul Integr Comp Physiol 287: R336–341.

16. Mousa SA, Shakibaei M, Sitte N, Schäfer M, Stein C (2004) Subcellular pathways of beta-endorphin synthesis, processing, and release from immuno-cytes in inflammatory pain. Endocrinology 145: 1331–1341.

17. Langenickel T, Pagel I, Höhnel K, Dietz R, Willenbrock R (2000) Differential regulation of cardiac ANP and BNP mRNA in different stages of experimental heart failure. Am J Physiol Heart Circ Physiol 278: H1500–1506.

18. Huang M, LeBlanc MH, Hester RL (1994) Evaluation of the needle technique for producing an arteriovenous fistula. J Appl Physiol 77: 2907–2911.

19. Abassi Z, Goltsman I, Karram T, Winaver J, Hoffman A (2011) Aortocaval fistula in rat: a unique model of volume-overload congestive heart failure and cardiac hypertrophy. J Biomed Biotechnol 2011:729497.

20. Goltsman I, Wang X, Lavallie ER, Diblasio-Smith EA, Ovcharenko E, et al. (2011) Effects of chronic rosiglitazone treatment on renal handling of salt and water in rats with volume-overload congestive heart failure. Circ Heart Fail 4: 345–354.

21. Chen Y-W, Pat B, Gladden JD, Zheng J, Powell P, et al. (2011) Dynamic molecular and histopathological changes in the extracellular matrix and inflammation in the transition to heart failure in isolated volume overload. Am J Physiol Heart Circ Physiol 300: H2251–2260.

22. Frederick JR, Fitzpatrick JR, McCormick RC, Harris DA, Kim A-Y, et al. (2010) Stromal cell-derived factor-1alpha activation of tissue-engineered endothelial progenitor cell matrix enhances ventricular function after myocardial infarction by inducing neovasculogenesis. Circulation 122: S107–117.

23. Murray DB, Gardner JD, Brower GL, Janicki JS (2008) Effects of nonselective endothelin-1 receptor antagonism on cardiac mast cell-mediated ventricular remodeling in rats. Am J Physiol Heart Circ Physiol 294: H1251–1257.

24. Berthiaume JM, Bray MS, McElfresh TA, Chen X, Azam S, et al. (2010) The myocardial contractile response to physiological stress improves with high saturated fat feeding in heart failure. Am J Physiol Heart Circ Physiol 299: H410–421.

25. Flaim SF, Minteer WJ, Nellis SH, Clark DP (1979) Chronic arteriovenous shunt: evaluation of a model for heart failure in rat. Am J Physiol 236: H698–704.

26. Hutchinson KR, Guggilam A, Cismowski MJ, Galantowicz ML, West TA, et al. (2011) Temporal pattern of left ventricular structural and functional remodeling following reversal of volume overload heart failure. J Appl Physiol 111: 1778–1788.

27. Apostolakis S, Lip GYH, Shantsila E (2009) Monocytes in heart failure: Relationship to a deteriorating immune overreaction or a desperate attempt for tissue repair? Cardiovasc Res 85: 649–660.

28. Searle J, Danne O, Müller C, Mockel M (2011) Biomarkers in acute coronary syndrome and percutaneous coronary intervention. Minerva Cardioangiol 59: 203–223.

29. Böhm M, Voors AA, Ketelslegers J-M, Schirmer SH, Turgonyi E, et al. (2011) Biomarkers: optimizing treatment guidance in heart failure. Clin Res Cardiol 100: 973–981.

30. Palazzuoli A, Caputo M, Calabró A, Nuti R (2010) Clinical impact of BNP and other emerging biomarkers in heart failure evaluation and management. Minerva Cardioangiol 60: 183–194.

31. Takeda Y, Fukutomi T, Suzuki S, Yamamoto K, Ogata M, et al. (2004) Effects of carvedilol on plasma B-type natriuretic peptide concentration and symptoms in patients with heart failure and preserved ejection fraction. Am J Cardiol 94: 448–453.

32. Dorn GW (2009) Apoptotic and non-apoptotic programmed cardiomyocyte death in ventricular remodeling. Cardiovasc Res 81: 465–473.

33. Khoynezhad A, Jalali Z, Tortolani AJ (2007) A synopsis of research in cardiac apoptosis and its application to congestive heart failure. Tex Heart Inst J 34: 352–359.

34. Lee Y, Gustafsson AB (2009) Role of apoptosis in cardiovascular disease. Apoptosis 14: 536–548.

35. Abbate A, De Falco M, Morales C, Gelpi RJ, Prisco M, et al. (2007) Electron microscopy characterization of cardiomyocyte apoptosis in ischemic heart disease. Int J Cardiol 114: 118–120.

36. Fu HY, Okada K, Liao Y, Tsukamoto O, Isomura T, et al. (2010) Ablation of C/EBP homologous protein attenuates endoplasmic reticulum-mediated apoptosis and cardiac dysfunction induced by pressure overload. Circulation 122: 361–369.

37. Dent MR, Das S, Dhalla NS (2007) Alterations in both death and survival signals for apoptosis in heart failure due to volume overload. J Mol Cell Cardiol 43: 726–732.

38. Chen Y-W, Pat B, Gladden JD, Zheng J, Powell P, et al. (2011) Dynamic molecular and histopathological changes in the extracellular matrix and inflammation in the transition to heart failure in isolated volume overload. Am J Physiol Heart Circ Physiol 300: H2251–2260.

39. Bristow MR, Ginsburg R, Minobe W, Cubicciotti RS, Sageman WS, et al. (1982) Decreased catecholamine sensitivity and beta-adrenergic-receptor density in failing human hearts. N Engl J Med 307: 205–211.

40. Chidsey CA, Braunwald E, Morrow AG, Mason DT (1963) Myocardial norepinephrine concentration in man. Effects of reserpine and of congestive heart failure. N Engl J Med 269: 653–658.

41. Cohn JN, Levine TB, Olivari MT, Garberg V, Lura D, et al. (1984) Plasma norepinephrine as a guide to prognosis in patients with chronic congestive heart failure. N Engl J Med 311: 819–823.

42. Hasking GJ, Esler MD, Jennings GL, Burton D, Johns JA, et al. (1986) Norepinephrine spillover to plasma in patients with congestive heart failure: evidence of increased overall and cardiorenal sympathetic nervous activity. Circulation 73: 615–621.

43. Leimbach WN, Wallin BG, Victor RG, Aylward PE, Sundlöf G, et al. (1986) Direct evidence from intraneural recordings for increased central sympathetic outflow in patients with heart failure. Circulation 73: 913–919.

44. Hammond HK, Roth DA, Insel PA, Ford CE, White FC, et al. (1992) Myocardial beta-adrenergic receptor expression and signal transduction after chronic volume-overload hypertrophy and circulatory congestion. Circulation 85: 269–280.

45. Böhm M, Lohse MJ (1994) Quantification of beta-adrenoceptors and beta-adrenoceptor kinase on protein and mRNA levels in heart failure. Eur Heart J 15 Suppl D: 30–34.

46. Ihl-Vahl R, Eschenhagen T, Kübler W, Marquetant R, Nose M, et al. (1996) Differential regulation of mRNA specific for beta 1- and beta 2-adrenergic receptors in human failing hearts. Evaluation of the absolute cardiac mRNA levels by two independent methods. J Mol Cell Cardiol 28: 1–10.

47. Gauthier C, Leblais V, Kobzik L, Trochu JN, Khandoudi N, et al. (1998) The negative inotropic effect of beta3-adrenoceptor stimulation is mediated by activation of a nitric oxide synthase pathway in human ventricle. J Clin Invest 102: 1377–1384.

48. Cheng HJ, Zhang ZS, Onishi K, Ukai T, Sane DC, et al. (2001) Upregulation of functional beta(3)-adrenergic receptor in the failing canine myocardium. Circ Res 89: 599–606.

49. Gauthier C, Sèze-Goismier C, Rozec B (2007) Beta 3-adrenoceptors in the cardiovascular system. Clin Hemorheol Microcirc 37: 193–204.

50. Moniotte S, Kobzik L, Feron O, Trochu JN, Gauthier C, et al. (2001) Upregulation of beta(3)-adrenoceptors and altered contractile response to inotropic amines in human failing myocardium. Circulation 103: 1649–1655.